DETECTION OF SIGNALS IN NOISE USING SINGLE CHANNEL RECEIVERS

John Lowell Bilodeau

NAVAL POSTGRADUATE SCHOOL
Monterey, California

THESIS

DETECTION OF SIGNALS IN NOISE
USING SINGLE CHANNEL RECEIVERS

by

John Lowell Bilodeau

December 1975

Thesis Advisor: G. A. Myers

Prepared for:

MCT SSA
PLRS Unit
Camp Pendleton, CA 92055

NAVAL POSTGRADUATE SCHOOL
Monterey, California

Rear Admiral Isham Linder
Superintendent

Jack R. Borsting
Provost

This thesis prepared in conjunction with research supported in part by the Naval Postgraduate School.

Released as a
Technical Report by:

REPORT DOCUMENTATION PAGE		READ INSTRUCTIONS BEFORE COMPLETING FORM
1. REPORT NUMBER	2. GOVT ACCESSION NO.	3. RECIPIENT'S CATALOG NUMBER
4. TITLE (and Subtitle) Detection of Signals in Noise Using Single Channel Receivers		5. TYPE OF REPORT & PERIOD COVERED 1 Jan 1975 - 1 Dec 1975 6. PERFORMING ORG. REPORT NUMBER
7. AUTHOR(s) John Lowell Bilodeau in conjunction with Glen A. Myers		8. CONTRACT OR GRANT NUMBER(s)
9. PERFORMING ORGANIZATION NAME AND ADDRESS Naval Postgraduate School Monterey, California 93940		10. PROGRAM ELEMENT, PROJECT, TASK AREA & WORK UNIT NUMBERS WR 5-0091
11. CONTROLLING OFFICE NAME AND ADDRESS Naval Postgraduate School Monterey, California 93940		12. REPORT DATE December 1975 13. NUMBER OF PAGES 43
14. MONITORING AGENCY NAME & ADDRESS(if different from Controlling Office) Marine Corps Tactical Systems Support Activity PLRS Unit Camp Pendleton, CA 92055		15. SECURITY CLASS. (of this report) Unclassified 15a. DECLASSIFICATION/DOWNGRADING SCHEDULE

16. DISTRIBUTION STATEMENT (of this Report)

Approved for public release; distribution unlimited .

17. DISTRIBUTION STATEMENT (of the abstract entered in Block 20, if different from Report)

18. SUPPLEMENTARY NOTES

19. KEY WORDS (Continue on reverse side if necessary and identify by block number)

Spread Spectrum
Direction Finding

20. ABSTRACT (Continue on reverse side if necessary and identify by block number)

A single-channel receiving system capable of detecting low power signals and of determining their angle of arrival is presented. The technique is based on the correlation of a signal with its reflection. The effect of noise is considered, and the feasibility of detecting a signal for which the autocorrelation is known is given. The description of a practical system which was constructed is provided, and

(20. ABSTRACT Continued)

the results of operation of this receiving system in the UHF band are presented.

Detection of Signals in Noise Using Single Channel Receivers

by

John Lowell Bilodeau
Captain, United States Marine Corps
B.S., Auburn University, 1967

Submitted in partial fulfillment of the
requirements for the degree of

MASTER OF SCIENCE IN ELECTRICAL ENGINEERING

from the

NAVAL POSTGRADUATE SCHOOL
December 1975

ABSTRACT

A single-channel receiving system capable of detecting low power signals and of determining their angle of arrival is presented. The technique is based on the correlation of a signal with its reflection. The effect of noise is considered, and the feasibility of detecting a signal for which the autocorrelation is known is given. The description of a practical system which was constructed is provided, and the results of operation of this receiving system in the UHF band are presented.

TABLE OF CONTENTS

LIST OF FIGURES

LIST OF SYMBOLS

c	Speed of light
d	Distance between antennas, or distance between antenna and reflector
f	Cutoff frequency of lowpass filter
k	Constant
ℓ	Length of reflector
m	Minimum ratio of terms required for detection
$n(t)$	Thermal noise
p	Path length difference
$s(t)$	Signal voltage as a function of time
t	Time
$v(t)$	Voltage as a function of time
$\overline{v(t)}$	Average of the voltage $v(t)$
v_o	Voltage output of the correlator
IF	Intermediate frequency (60 MHz)
RC	Resistor-capacitor
RF	Radio frequency
$R_{ss}(\tau)$	Autocorrelation function of $s(t)$
T	Delay caused by path length difference
UHF	Ultra high frequency
α	Angle of arrival of the signal
α_m	Maximum angle of arrival of the signal
π	Pi
τ	Delay caused by circuit element

I. INTRODUCTION

This report is concerned with the detection of low power spread spectrum signals, and the determination of the angle of arrival of such signals. Presented is a technique using a single receiver for accomplishing both of these tasks.

Spread spectrum signals have their energy intentionally distributed over a bandwidth much greater than the bandwidth of the transmitted message. In some applications, the power level of the signal is less than that of thermal noise. This prevents detection of the signal by normal threshold decision means. Cooperative receivers use cross-correlation techniques to recover such signals. A priori information of the structure of the signal allows the cooperative receiver to duplicate or store the signal and thereby correlate to detect the energy and recover the transmitted data. [Ref. 1]

Uncooperative receivers do not have a replica of the signal and so cross-correlation techniques are denied them. Autocorrelation techniques are possible as described next and in the remainder of this report. [Ref. 2]

Let a receiver input voltage $v(t)$ consist of a signal component $s(t)$ and additive noise $n(t)$. This is, $v(t) = s(t) + n(t)$. Squaring this voltage gives

$$v^2(t) = s^2(t) + 2s(t)n(t) + n^2(t) \qquad (1)$$

Lowpass filtering has the effect of integrating or averaging a signal. The effect of lowpass filtering the product extracts the DC component with the result that

$$\overline{v^2(t)} = \overline{s^2(t)} + \overline{n^2(t)} \qquad (2)$$

where $\bar{x}$ denotes the average value of x. Here it is assumed $\overline{s(t)n(t)} = 0$ which is true whenever s(t) and n(t) are uncorrelated (from different sources).

Now in the absence of noise, the lowpass filter output is $\overline{s^2(t)}$, a measure of the average power of the received signal. The presence of a signal is then determined by inspecting the lowpass filter output. In the presence of noise, this filter output is not always a reliable indicator of signal presence because for small ratios of signal power to noise power (SNR) the noise dominates the output and masks the presence of a signal. For this reason simple product detectors are not generally effective when the SNR is small (< 1).

What is required is a means of reducing the noise term while preserving the coherence of the signal component. One method is to use two receiving channels. Each channel receives the same signal component, but each generates different, uncorrelated noise terms. The product then becomes

$$v_1(t)\ v_2(t) = [s(t) + n_1(t)]\ [s(t) + n_2(t)] \qquad (3)$$

which after filtering reduces to

$$\overline{v_1(t)\ v_2(t)} = \overline{s^2(t)} \tag{4}$$

This system can in theory detect any signal independent of the noise levels. Limitations are those associated with measurements and maximum integration time available.

In the next section, there is a discussion of how these two-channel systems can be implemented to indicate angle of arrival of the signal. The development leads to consideration of a single-channel receiving system which can be used to detect weak signals and indicate their angle of arrival. This single channel system is the subject of this report.

II. DIRECTION-FINDING CORRELATION TECHNIQUES

A. GENERAL DESCRIPTION

First consider a two element interferometer which uses a correlator to produce an output v_o dependent upon the direction of arrival of the received signal. A typical system employes two antennas separated by a distance d as shown in Fig. 1. Each antenna has an associated receiving system comprised of RF amplification, frequency selection and IF amplification sections. The incoming signal arrives at one antenna T seconds before it arrives at the second antenna. The output of the first antenna is delayed for τ seconds and then applied to the first port of the correlator. The output of the second antenna is applied directly to the second port of the correlator. The output v_o of the correlator is then

$$v_o = \overline{v_1(t-\tau)\ v_2(t)} \tag{5}$$

where

$$v_1 = s(t) + n_1(t) \tag{6}$$

and

$$v_2 = s(t-\tau) + n_2(t) \tag{7}$$

Appendix A presents the development of the relation between T and the angle of arrival. From Equ. A-1

$$T = \frac{d \sin \alpha}{c} \tag{8}$$

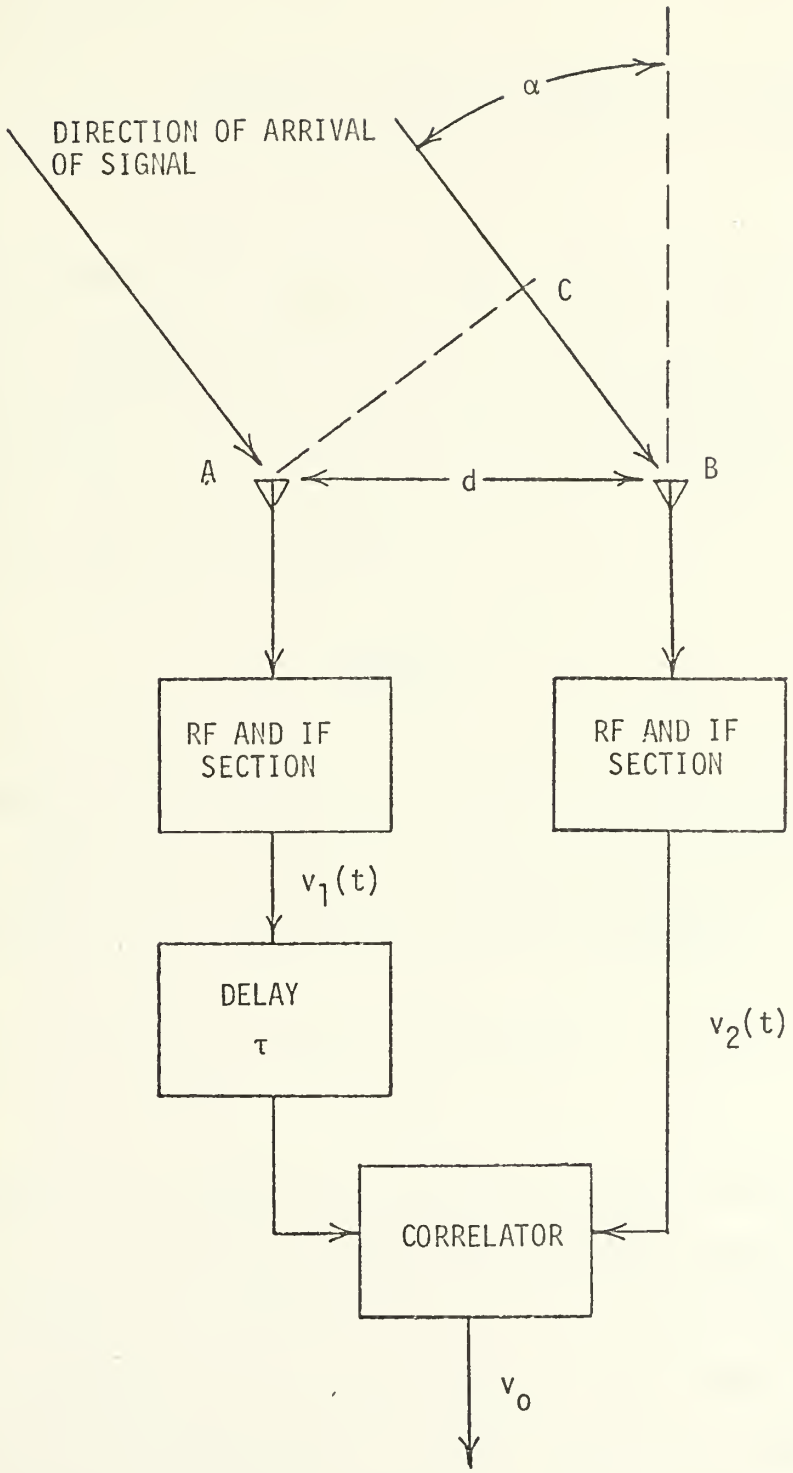

FIG. 1. Block diagram of a parallel channel system.

where α is the angle of arrival as shown in Fig. 1 and c is the speed of light.

Then

$$v_o = \overline{[s(t-\tau) + n_1(t-\tau)]\,[s(t-T) + n_2(t)]} \qquad (9)$$

When the delay τ is equal to the time of arrival difference T of the incoming signals, the correlation of the signals v_o is at its maximum value (signal components are "in phase"). The direction of arrival is then determined as follows.

From Appendix A equation A-1

$$T = \frac{d \sin \alpha}{c}$$

To determine the angle of arrival of the incoming signal, adjust the delay τ until the correlator output v_o is maximized, (τ=T), and apply the relationship

$$\alpha = \sin^{-1} \frac{cT}{d} = \sin^{-1} \frac{c\tau}{d} \qquad (10)$$

There is a practical difficulty with a parallel channel system. The frequency selection and amplification section of the separate channels must be very nearly identical. Even small amounts of distortion in one of the channels may prevent the correlation function from being maximized at the proper delay and will introduce errors in angle of arrival

information as well as a loss of sensitivity. Therefore, the two channel receiving system must be gain and phase matched over its entire operating range of frequencies. To avoid these practical difficulties of parallel-channel systems, means of correlation detection using single-channel receivers were investigated.

Consider replacing one of the antennas by a reflector arranged so that a signal will travel to the reflector and be returned to the remaining antenna with a relative delay of T seconds. This would provide a single signal of $s(t) + k\ s(t-T)$ where the constant k accounts for the losses during reflection. The configuration is as shown in Fig. 2.

Included in the RF and IF sections of Fig. 2 are a radio frequency amplifier, a mixer and local oscillator, and an IF amplifier. This configuration places the reflector directly behind the single antenna. This results in the shortest physical separation for a given delay. The path length difference p is from Equ. A-2 of Appendix A,

$$p = 2\ d \cos \alpha$$

and the delay T between the incident and reflected signal is

$$T = \frac{p}{c} = \frac{2d}{c} \cos \alpha \quad . \tag{11}$$

Then

$$v_1(t) = s(t) + k\ s(t-T) \quad . \tag{12}$$

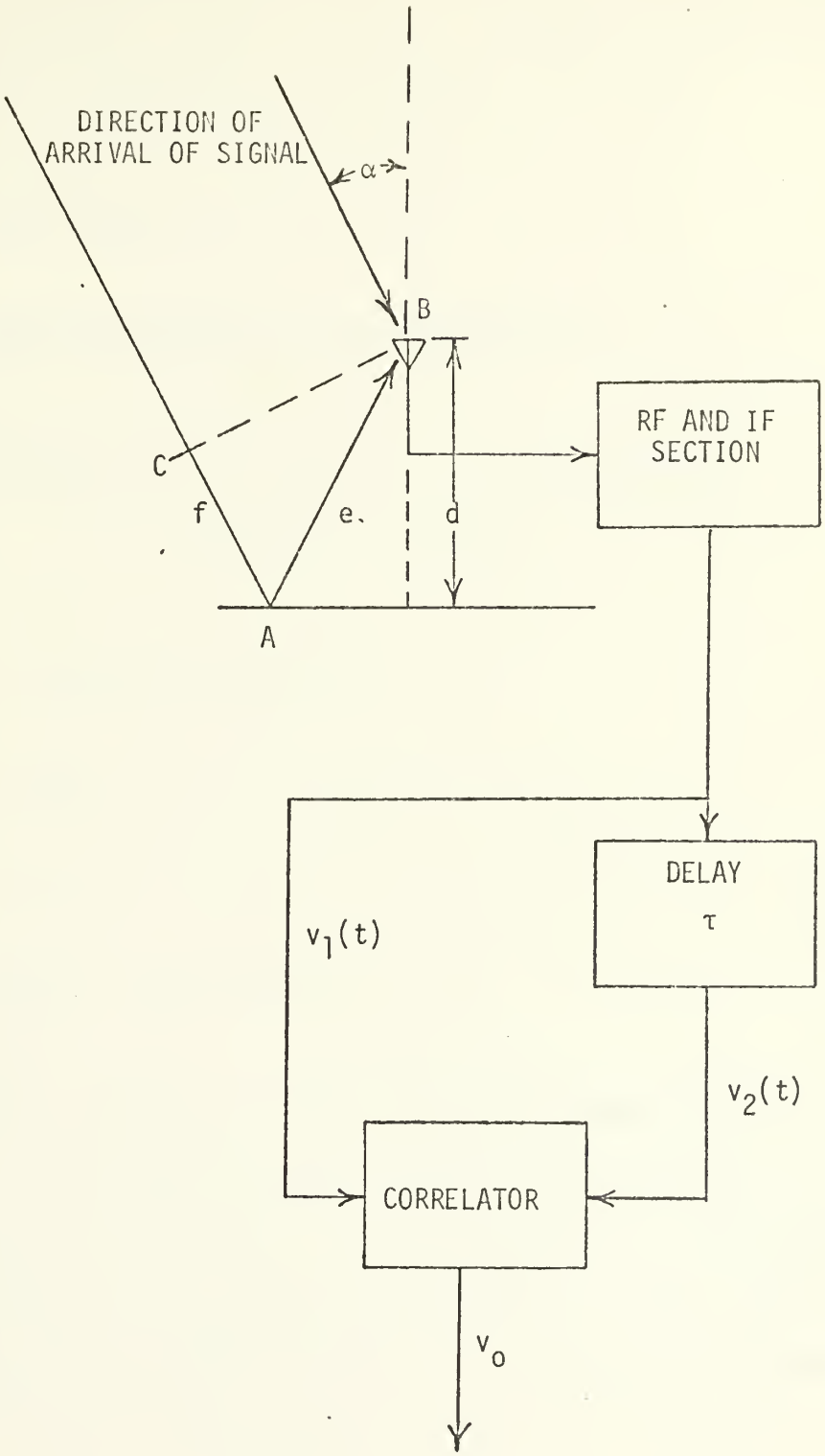

FIG. 2. Block diagram of a single channel system with back reflector.

If $v_1(t)$ is applied to one port of the correlator and a delayed version, $v_2(t) = v_1(t-\tau)$ applied to the second port of the correlator, the output v_o will be

$$v_o = \overline{v_1(t)\ v_2(t)} \tag{13}$$

$$v_o = \overline{[s(t) + ks(t-T)][s(t-\tau) + ks(t-T-\tau)]} \tag{14}$$

$$v_o = \overline{s(t)s(t-T) + s(t)\ k\,s(t-T-\tau) + k\,s(t-T)\,s(t-\tau) + k^2\,s(t-T)\,s(t-T-\tau)} \tag{15}$$

Assuming stationarity [Ref. 3]

$$v_o = (1 + k^2)\ R_{ss}(\tau) + k\,R_{ss}(\tau+T) + k\,R_{ss}(\tau-T) \tag{16}$$

where

$$R_{ss}(\tau) = \overline{s(t)\ s(t-\tau)} \tag{17}$$

The addition of noise is not considered here but will be included at the end of this section. The criterion for neglecting $(1 + k^2)\ R_{ss}(\tau)$ and $k\,R_{ss}(\tau+T)$ are presented in the next section, but assuming they can be neglected, then $v_o = k\,R_{ss}(\tau-T)$. When the delay τ is adjusted to equal T we have

$$v_o = k\,R_{ss}(0) \tag{18}$$

Since $R_{ss}(0)$ is the maximum value of $R_{ss}(\tau)$ it is only necessary to adjust the delay τ until v_o is maximized and apply equation A-3 to find α as

$$\alpha = \cos^{-1} \frac{Tc}{2d} = \cos^{-1} \frac{\tau c}{2d} \quad . \tag{19}$$

To determine the sensitivity of T to a change in α, differentiate equ. A-3 to obtain

$$\frac{dT}{d\alpha} = \frac{d(2d \cos \alpha)}{d\alpha} = -2d \sin \alpha \tag{20}$$

$$\left.\frac{dT}{d\alpha}\right|_{\alpha=0} = -2d \sin 0 = 0 \tag{21}$$

which shows the sensitivity of T to a change in α is a minimum when $\alpha = 0$. In general this is a disadvantage of the geometry of Fig. 2.

Another geometry is now considered which will increase the sensitivity of T to α. Placing the reflector on a line perpendicular to the direction of arrival of the signal and set at a 45 degree angle to this line as shown in Fig. 3 provides a path length difference

$$p = d \left[\frac{1 + 2 \sin \alpha \cos \alpha}{\cos \alpha + \sin \alpha} \right]$$

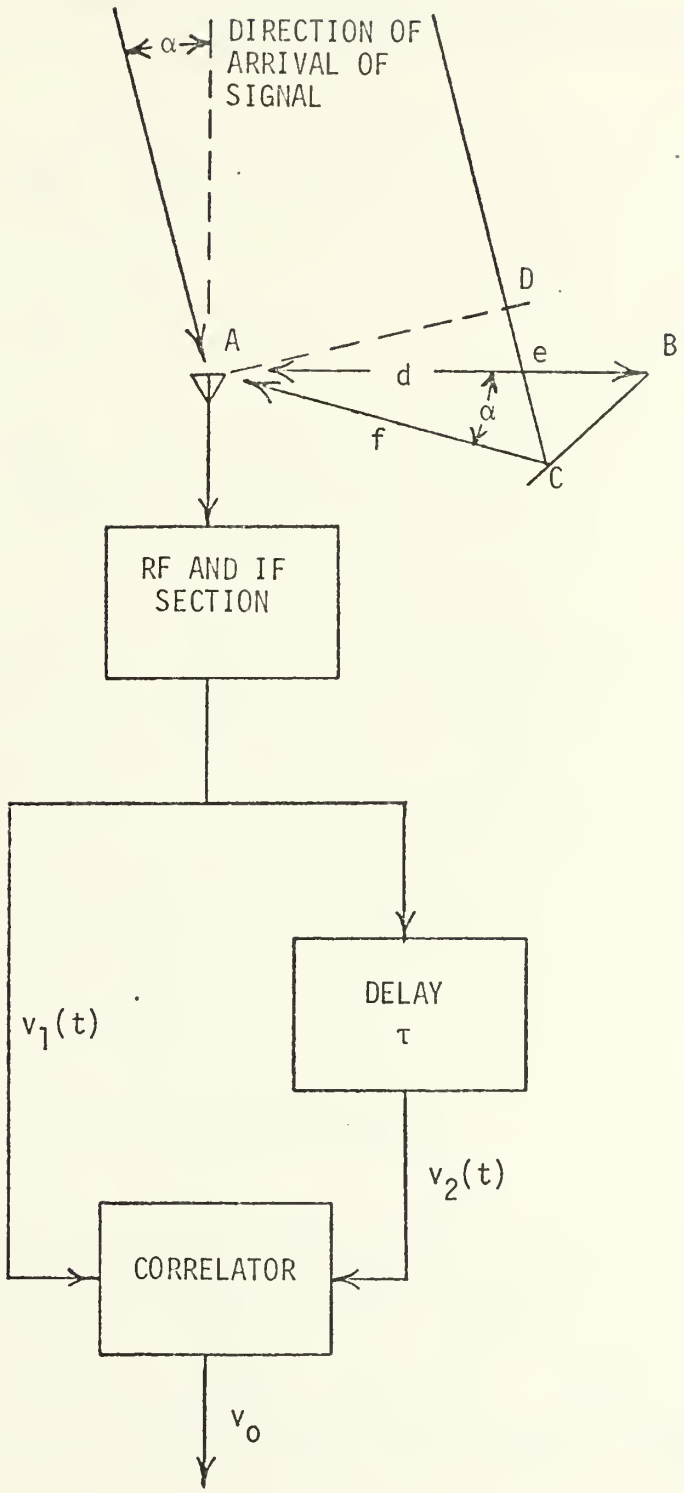

FIG. 3. Block diagram of a single channel system with side reflector.

which is derived in Appendix A. The sensitivity of the path length difference to a change in α becomes

$$\frac{dp}{d\alpha} = \frac{d(2\cos^2\alpha + 2\sin^2\alpha)(\cos\alpha + \sin\alpha) - (1 + 2\sin\alpha\cos\alpha)(\cos\alpha - \sin\alpha)}{(\cos\alpha + \sin\alpha)^2} \qquad (22)$$

$$\frac{dp}{d\alpha} = d(\cos\alpha - \sin\alpha) \qquad (23)$$

Evaluating at $\alpha = 0$ gives

$$\left.\frac{dp}{d\alpha}\right|_{\alpha=0} = d(\cos 0 - \sin 0) = d \quad . \qquad (24)$$

The minimum length of the reflector can be determined from geometric considerations by finding the length required to just intercept a ray from an infinite source which will reflect to the receiving antenna if its angle of arrival is α_m. Let ℓ be the required length of the reflector. Then from Appendix A Equ. A-5,

$$\ell = d\,\frac{\sin\alpha_m}{\sin(135 - \alpha_m)} \qquad (25)$$

where α_m is the maximum angle of arrival of interest.

The maximum length of the reflector is limited by the near field effect of the reflection. As the reflector's length is increased the near field effect becomes more

prominent. As a rule of thumb, the near field is significant to a distance of $\frac{2\ell^2}{\lambda}$ units from the reflector where $\lambda = \frac{c}{f_c}$ and where c is the velocity of propagation and f_c the carrier frequency of the reflected signal. This effect causes the power reflected to change rapidly as a function of the angle of arrival. Further, operation in the near field may introduce distortion in the resultant reflected signal preventing correlation function maxima from occurring at the predicted value of τ.

B. REQUIREMENTS FOR THE NOISELESS CASE

We can determine the required value of T needed to detect the signal by examining the correlator output v_o derived as Equ. 15 in the previous section. When τ is equal to T,

$$v_o = (1+k^2) R_{ss}(T) + k R_{ss}(0) + k R_{ss}(2T) \quad . \qquad (26)$$

The term of interest here is $k R_{ss}(0)$. The other terms act as interference which mask the term of interest. Choosing m to be the minimum ratio of these terms which can be detected, then

$$m \leq \frac{k R_{ss}(0)}{(1+k^2) R_{ss}(T) + k R_{ss}(2T)} \qquad (27)$$

and

$$R_{ss}(0) \geq \frac{m}{k} [(1+k^2) R_{ss}(T) + k R_{ss}(2T)] \qquad (28)$$

insures a detectable response. The relationship of these terms is shown in Fig. 4.

Using this criterion and given the value of m and k, the distance d must be adjusted to result in T large enough to provide the required increase in the measured output of the correlator. From a knowledge of the shape of the auto-correlation function we can then determine the range through which τ must be varied for a detectable change in the correlator output and thus the accuracy to which α can be determined.

As an example of this technique, Figs. 5 and 6 show the result of a computer simulation where s(t) is a pulse. If the 200 nsec triangular pulse of Fig. 5A is received, the normalized curve of Fig. 5B indicates the correlator output as a function of τ. If this pulse is then reflected with T = 152 nsec and k = 0.5, the result is the pulse shown in Fig. 6A. This new pulse produces the normalized correlator output of Equ. (16) shown in Fig. 6B. A comparison of Figs. 5B and 6B indicates that $R_{ss}(T)$ where T is 152 nsec is somewhat less than $k R_{ss}(0)$. Since the effect of $k R_{ss}(0)$ is clearly visible in the area of τ = 152 nsec, it is clear that m is above the minimum value required for detection in this case.

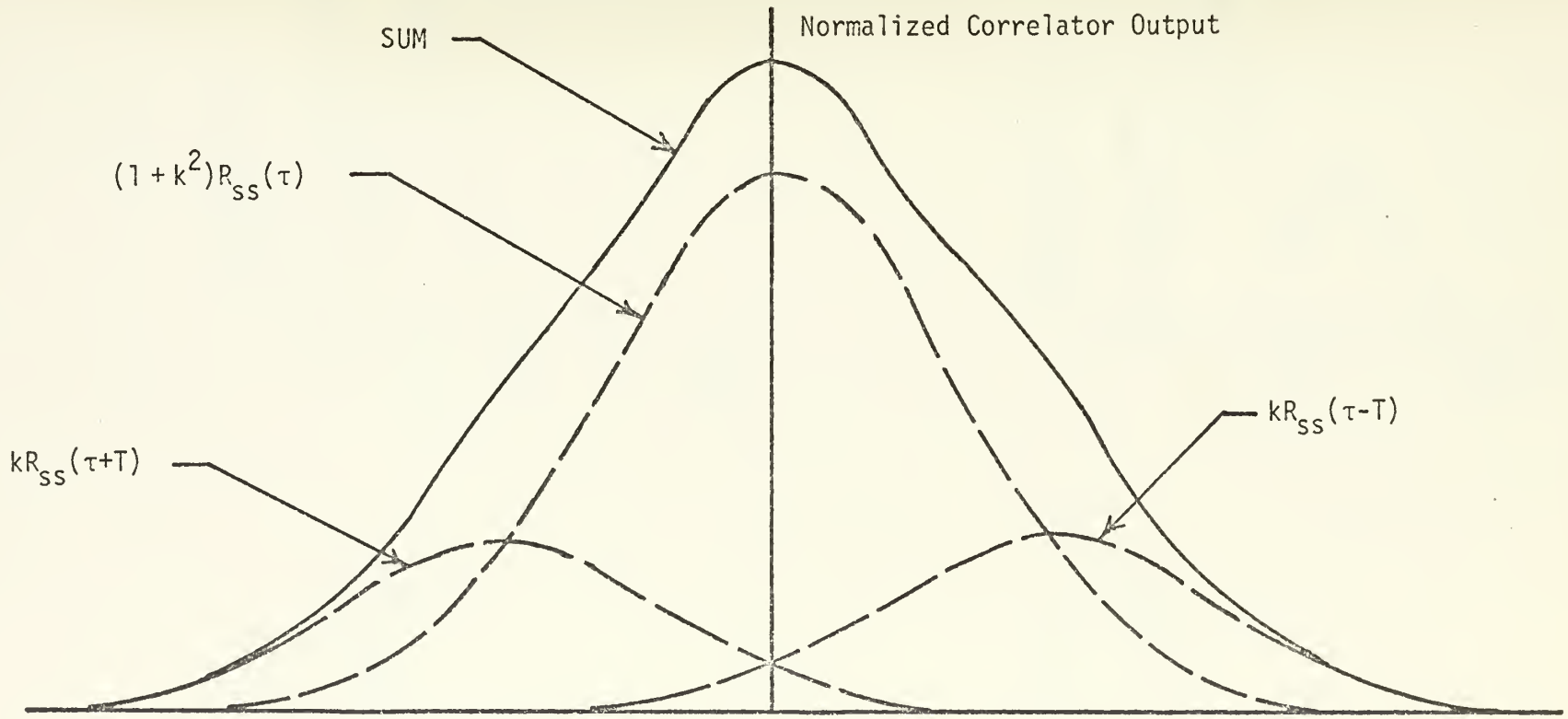

FIG. 4. The resultant autocorrelation function of the sum of a received signal and its reflection.

FIG. 5A

FIG. 5B

FIG. 6A

FIG. 6B

C. THE ADDITIVE NOISE CASE

The addition of noise complicates this problem. Since noise and signal are assumed to be uncorrelated, it is only necessary to insure that the autocorrelation function of the noise $R_{nn}(\tau)$ is below the detection criterion when $\tau = T$. This can be seen as follows. With noise present, the direct path voltage can be written as $s(t) + n(t)$. The correlator output becomes

$$v_o = [\overline{s(t) + k\,s(t-T) + n(t)}\ ]\ [s(t-\tau) + k\,s(t-T-\tau) + n(t-\tau)\ ] \qquad (29)$$

which reduces to

$$v_o = \overline{s(t-\tau)\ s(t)} + \overline{k\,s(t-\tau)\ s(t-T)} + \overline{k\,s(t-T-\tau)\ s(t)}$$

$$+ \overline{k\,s(t-T-\tau)\ s(t-\tau)} + \overline{n(t-\tau)\ n(t)} \quad . \qquad (30)$$

Assuming a rectangular lowpass noise spectrum of unity amplitude, then

$$R_{nn}(\tau) = \frac{\sin(\pi\tau f)}{\pi\tau} \qquad \text{where f is the upper frequency limit of the lowpass spectrum} \qquad (31)$$

Then when $\tau = T$

$$R_{nn}(T) = \frac{\sin(\pi T f)}{\pi T} < \frac{R_{ss}(0)}{m} \qquad (32)$$

is required for detection from Equ. 31.

Fortunately most spread spectrum signals are designed to have a rapidly decreasing autocorrelation function, and the wide bandwidth of the signal implies a receiver bandwidth such that the autocorrelation function of the noise can be well approximated to be that of Equ. 31.

III. A PRACTICAL SINGLE CHANNEL SYSTEM

A. GEOMETRY

The geometry of the receiving system used in this study is as shown in Fig. 3. The transmitter is placed approximately 600 feet from the receiver and on approximately the same elevation. The frequency selected for the test is 435 MHz because of the availability of low power spread spectrum transmitters at that frequency. The receiver antenna is separated a distance of 100 to 150 feet from the reflector. This results in a difference in time of arrival of approximately 100 to 150 nsec when the angle of arrival is zero.

It has been determined experimentally that delays in the order of 200 nsec can be achieved using RG58 coaxial cable. The maximum angle of arrival is chosen to be 12°. Using Equ. A-5 this results in a required reflector length of

$$\ell = \frac{100 \sin 12°}{\sin (127°)} = 26.0 \text{ ft.}$$

B. CONSTRUCTION OF THE REFLECTOR

Passive reflector technology is well developed in the microwave frequency region. The rules generally used in construction of these microwave reflectors require the reflecting face to be flat to a tolerance of 12.5 percent of a wavelength. At 435 MHz, this results in a required flatness accuracy of 8.62 cm.

The supporting structure for the reflector is constructed of wood. It is ten feet high and 30 feet long. The face of this support is covered by a tightly stretched wire mesh. The mesh size is approximately 2 cm. A type of wire mesh designed for caging birds referred to as "aviary wire" was selected. This wire mesh is galvanized after it has been fabricated insuring electrical continuity. The wire mesh is available in widths of three feet, so three 30 x 3 feet sections are joined along their long sides to cover the supporting frame. The junction of this wire mesh is soldered together every few inches to insure electrical continuity. The reflector is guyed in a vertical position as shown in Fig. 7.

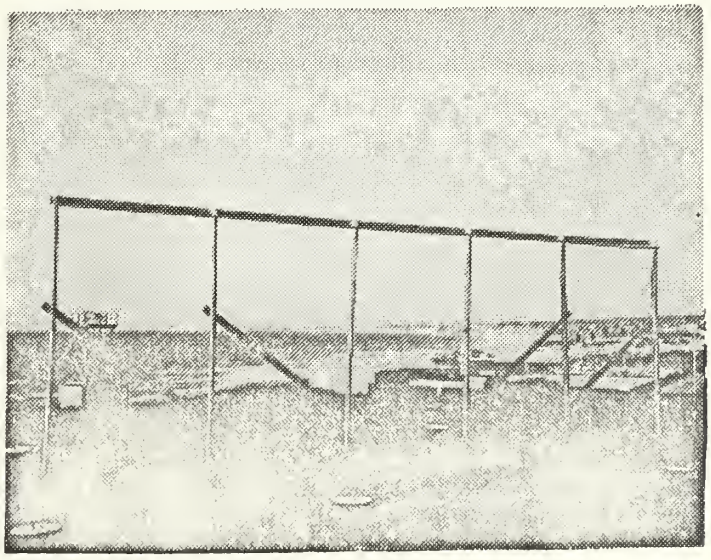

FIG. 7. The Nine by 30 Foot Reflector.

C. THE AMPLIFICATION AND FREQUENCY SELECTION SECTION

The frequency selection and amplification section are as shown in the block diagram of Fig. 8. This arrangement

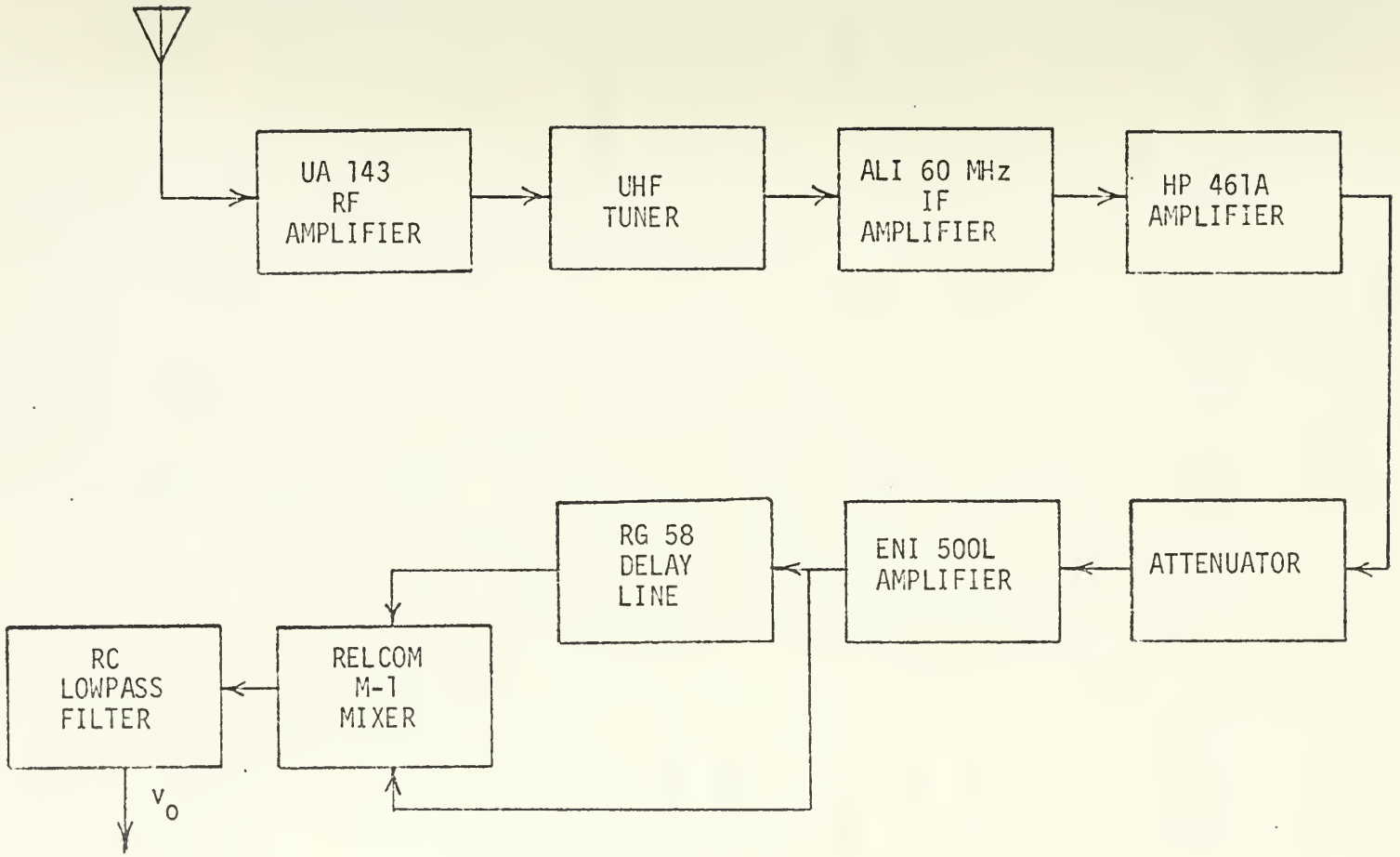

FIG. 8. Block diagram of the receiver.

provides a 10 MHz bandpass and the power levels to drive the correlator.

The antenna is a simple half wave monopole mounted above an aluminum ground plane. The base of the antenna is coupled directly to a coaxial connector which feeds the radio frequency amplifier.

The radio frequency amplifier is an Avantek UA-143 wide band amplifier. It provides 15 db of gain with a 2.5 db noise factor.

The tuner is a converted commercial UHF television tuner. It consists of a single transistor oscillator, a tuned loaded cavity radio frequency selector, and a single diode mixer. The tuner is broadband with a noticeable drift in frequency setting. Conversion to 435 MHz consisted of adjusting the reactive elements in the radio frequency cavity to lower its frequency response and adjusting the intermediate frequency selector elements to respond to 60 MHz.

The first intermediate frequency amplifier is a 60 MHz Cutler-Hammer amplifier. This reduces the bandwidth of the selected frequency to 10 MHz and provides 40 db of gain. This amplifier is provided with automatic gain control which improves the dynamic range of the system.

The next amplifier of Fig. 8 is a Hewlett Packard HP461A 1 kHz to 150 MHz amplifier. It is also operated at 60 MHz. This amplifier has the capability of either 20 or 40 db of gain. Normally, the 20 db setting is used.

The attenuator in Fig. 8 increases the dynamic range of the system by preventing saturation of the output amplifier during periods of high signal power.

The output amplifier is an Electronic Navigation Industry's 500L, 500 MHz amplifier with 27 db of gain. The output of this amplifier is sufficient to drive both ports of the mixer.

The delay element of the system is composed of RG58 coaxial cable. This cable delays electrical energy 1.54 nsec per foot of cable. The cable is divided into convenient lengths in order to use combinations of these lengths to provide the desired delay. The smallest increment is 1.4 nsec.

Voltage multiplication is accomplished with a Relcom M-1 0.2 to 500 MHz double-balanced mixer followed by an RC filter. Its wide bandwidth assures correlation at the intermediate frequency, and its 50 ohm impedance prevents reflections in the delay line. The RC lowpass filter completes the correlator section.

IV. RESULTS AND RECOMMENDATIONS

A. INITIAL TEST

The success of this system depended upon the efficiency of the reflector. Attempts to insure the reflectivity constant k were made by measuring the standing wave pattern in space in the area of the antenna. These measurements indicated a signal power "standing wave ratio" of approximately 8 db. Attempts were then made to operate the system.

A lack of success during this phase of operation led to the testing of the reflector by transmitting short pulses of radio frequency. When no reflection was observed with the short pulses a new geometry was attempted. This arrangement put the reflector directly behind the antenna and perpendicular to the transmitter antenna – receiver antenna axis as shown in Fig. 2. As previously indicated, this position gave very poor directional sensitivity, but it was felt that the greatest reflection could be realized. A short pulse of radio frequency was transmitted and resulted in a clear reflection. Fig. 9 is a photograph of an oscilloscope presentation of this reflection. The y axis is the envelope of the pulse. The y scale is 0.05 volts per cm, and the x scale is 100 nsec per cm. The receiving antennas was 75.0 feet in front of the reflector. From Equ. A-3, the delay realized is

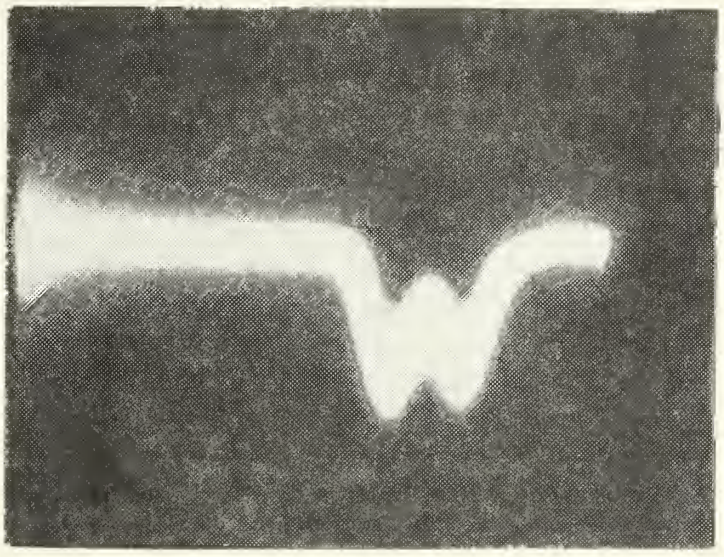

FIG. 9. Oscilloscope Presentation of a Pulse and its Reflection.

$$T = \frac{2d \cos \alpha}{c} = \frac{2 \times 75 \text{ ft.} \cos 0}{984 \times 10^6 \text{ ft/sec.}}$$

$$T = 152 \text{ nsec.}$$

As can be seen from Fig. 9 the reflection occurred at the computed delay.

The shape of the autocorrelation function of the RF Pulse is determined by measuring the voltages at the output of the correlator for different lengths of delay line. Fig. 10A is the autocorrelation of the radio frequency pulse without the reflector. Fig. 10B is the autocorrelation of the pulse with reflection. As can be observed by comparing these

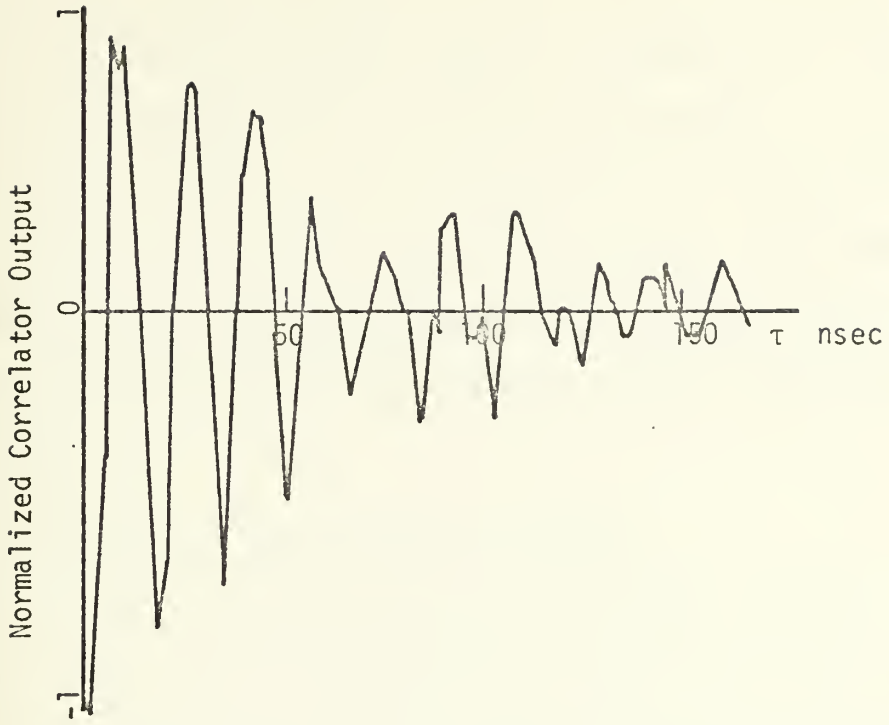

FIG. 10A. Correlation function of received signal without reflection.

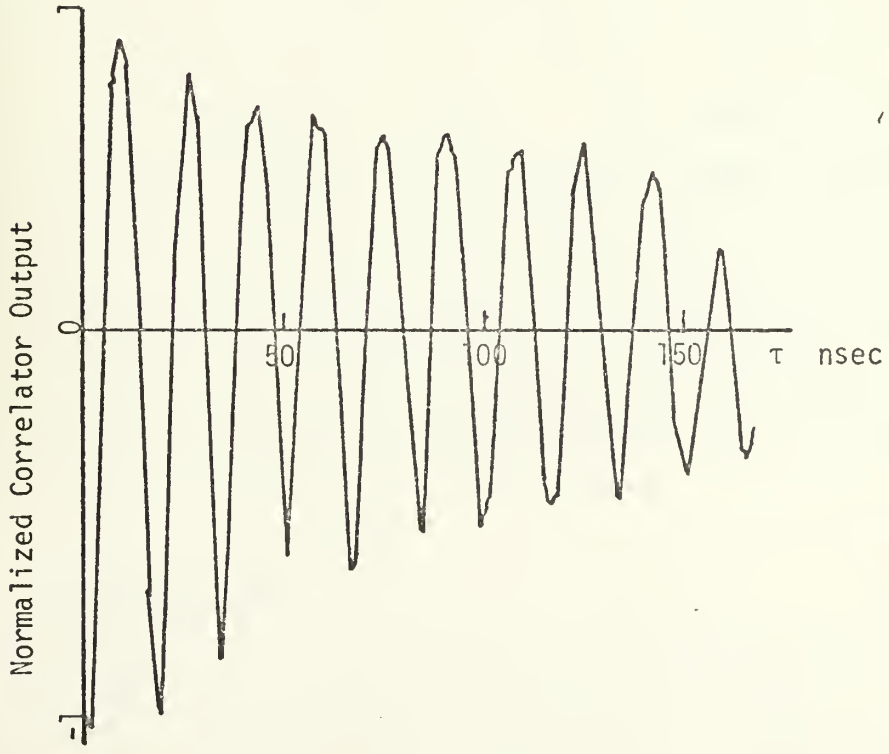

FIG. 10B. Correlation function of the sum of the incident signal and its reflection.

graphs with those of Figs. 5 and 6, the autocorrelation function of the reflected signal continues at a high level after that of the single pulse has decreased. The sinusoidal variation of these graphs is caused by the sinusoidal autocorrelation function of the IF frequency. The double balanced mixer was operated at 60 MHz output which produces a 60 MHz sinusoidal fine structure within the correlation envelope.

B. TEST WITH SPREAD SPECTRUM SIGNALS

Finally the system was tested against a spread spectrum source. Several spread spectrum signals were used to determine the usefulness of the system as an energy detector. Spread spectrum signal with bandwidths wider, equal to, and narrower than 10 MHz were generated with both the reflector behind the antenna as in Fig. 2 and the reflector to the side of the antenna as in Fig. 3. The system was unable to detect these signals at power levels lower than could be detected using ordinary product detectors. While shifts in zero crossings of the autocorrelation function were detected at the proper delay, lack of frequency stability of the receiver local oscillator masked changes due to the reflected signal.

C. RECOMMENDATIONS

Continuation of this project is recommended. Several areas of the system require refinement in order to obtain

more meaningful results. With the addition of the following refinements it appears that measurements of very low power signals will be possible.

1. The reflector requires a longer effective length. The short length of the reflector, approximately 13.3 wavelengths, causes the reflected signal to spread as it travels away from the reflecting surface. It would appear that the simplest method of accomplishing this is to increase the frequency at which the experiments are performed. This has the effect of making the reflector a greater number of wavelengths long and decreases the spreading effect of the reflector.

2. The local oscillator of the receiver should be stabilized. Frequency changes of a few percent in the local oscillator change the autocorrelation function of the signal so that it becomes difficult to determine which effects are due to frequency drift and which are due to reflection.

3. Correlation should be accomplished at base band rather than IF. This will result in elimination of the sinusoidal fine structure within the envelope of the correlation function and permit clearer observation of the change in correlation output when a reflection occurs.

D. ANOTHER APPLICATION

An interesting result was observed when using this system. When the signal is received without reflection, the autocorrelation function can be determined by changing the

delay τ and observing v_o. If two signals are present each with different autocorrelation function, they can be separated by adjusting the delay until one has a negative correlation and the other a positive correlator output. This can be observed from Fig. 11 where the signal of interest was a 10 MHz bandwidth spread spectrum signal while an interfering air search radar of unknown bandwidth but with overlapping frequencies exhibits a negative correlation. The first pulse of this photograph is the signal of interest. All others are from the radar. The delay in this case was 171.5 nsec.

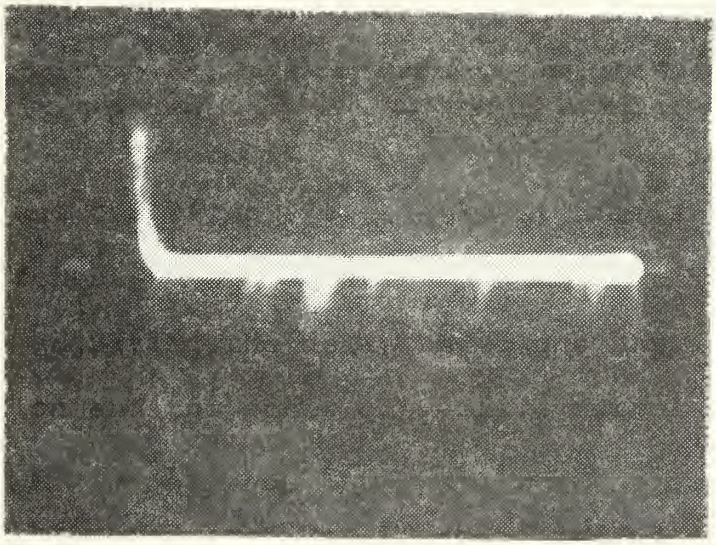

Fig. 11. Positive and negative correlating pulses

APPENDIX A

Appendix A contains the mathematical development of path length difference and delay for each of the three cases considered; (1) the parallel channel interferometer, (2) the back reflector case of Fig. 2, and (3) the side reflector case of Fig. 3. This appendix also contains the geometric consideration determining the length of the reflector for the side reflector case.

1. THE PARALLEL CHANNEL INTERFEROMETER

From Fig. 2 angle BAC = α since angles formed by mutually perpendicular lines are equal, and

$$p = d \sin \alpha$$

since ABC is a right triangle, where p is the path length difference. Therefore

$$T = \frac{p}{c} = \frac{d \sin \alpha}{c} \qquad \text{(A-1)}$$

where c is the speed of light, and T is the delay time.

2. THE BACK REFLECTOR

From Fig. 2

$$e = \frac{d}{\cos \alpha}$$

because ABD is a right triangle and

$$f = e \cos 2\alpha$$

because ABC is a right triangle, but

$$p = e + f$$

or

$$p = \frac{d}{\cos \alpha} + \frac{d \cos 2\alpha}{\cos \alpha}$$

or

$$p = \frac{d}{\cos \alpha} (1 + \cos 2\alpha) \quad .$$

Using trigonometric identities,

$$p = \frac{d}{\cos \alpha} (1 + 2 \cos^2 \alpha - 1)$$

$$p = \frac{d}{\cos \alpha} 2 \cos^2 \alpha = 2d \cos \alpha \qquad \text{(A-2)}$$

Hence

$$T = \frac{p}{c} = \frac{2d \cos \alpha}{c} \qquad \text{(A-3)}$$

3. THE SIDE REFLECTOR

From Fig. 3, consider triangle BCA where angle ABC = 45°, and angle ACB = 135°- α since the angle of incidence equals the angle of reflection. Angle CAB = α since the sum of the angles of a triangle is 180°.

Then

$$\frac{f}{\sin 45°} = \frac{d}{\sin(135°-\alpha)}$$

from the law of sines, or

$$f = \frac{d \sin 45°}{\sin(135°-\alpha)}$$

or

$$f = \frac{d \sin 45°}{\cos 45° \cos \alpha + \sin 45° \sin \alpha}$$

But

$$\sin 45° = \cos 45°$$

and so

$$f = \frac{d}{\cos \alpha + \sin \alpha}$$

Now consider triangle ACD.

Angle ADC = 90° by construction and

angle ACD = 180° - 2(α+45°) by symmetry.

Also

$$e = f \cos(180° - 2(\alpha+45°))$$

hence ACD is a right triangle, or

$$e = f \cos(90-2\alpha) = \sin 2\alpha \ .$$

But $p = e + f$

and so

$$p = d \frac{1 + 2 \sin \alpha \cos \alpha}{\cos \alpha + \sin \alpha} \qquad \text{(A-4)}$$

Therefore,

$$T = \frac{p}{c} = \frac{d}{c} \frac{1 + 2 \sin \alpha \cos \alpha}{\cos \alpha + \sin \alpha}$$

4. GEOMETRIC CONSIDERATIONS OF REQUIRED REFLECTOR LENGTH FOR THE SIDE REFLECTOR

Let α_m be the maximum angle of arrival of interest. Then when $\alpha = \alpha_m$, from Fig. 3 it is obvious that

$$\text{angle ACB} = 180° - (45°+\alpha_m)$$

and $$\text{angle CAB} = \alpha_m \ .$$

But

$$\frac{\ell}{\sin \alpha_m} = \frac{d}{\sin(180° - (45°+\alpha_m))}$$

from the law of sines where ℓ is the reflector length.

Rewriting gives

$$\ell = \frac{d \sin \alpha_m}{\sin(135°-\alpha_m)} \quad . \qquad \text{(A-5)}$$

LIST OF REFERENCES

1. Dillard, R. A., Vulnerability of Low-Detectability Communications to Energy Detection, Naval Electronics Laboratory Center, 26 Jan. 1975.

2. Naval Electronics Laboratory Center Technical Document 271, Proceedings of the 1973 Symposium on Spread Spectrum Communications, 13 March 1973.

3. Thomas, John B., An Introduction to Statistical Communications Theory, Wiley, 1969.

INITIAL DISTRIBUTION LIST

		No. Copies
1.	Defense Documentation Center Cameron Station Alexandria, Virginia 22314	2
2.	Library, Code 0212 Naval Postgraduate School Monterey, California 93940	2
3.	Department Chairman, Code 52 Department of Electrical Engineering Naval Postgraduate School Monterey, California 93940	2
4.	Associate Professor Glen Myers, Code 52Mv Department of Electrical Engineering Naval Postgraduate School Monterey, California 93940	5
5.	Associate Professor John Bouldry, Code 52Bo Department of Electrical Engineering Naval Postgraduate School Monterey, California 93940	1
6.	Argo Systems 1069 East Meadow Circle Palo Alto, California 94302 Attn: Mr. Jim de Broekart	1
7.	ESL, Inc. 495 Java Drive Sunnyvale, California 94086 Attn: Mr. William J. Phillips	1
8.	Commander Naval Security Group Command 3801 Nebraska Avenue, N.W. Washington, D.C. 20390	1
9.	Marine Corps Tactical Systems Support Activity P.L.R.S. Unit Camp Pendleton, California 92055 Attn: Maj. Norb Spitzer.	1
10.	Capt. John L. Bilodeau, USMC Development Center Marine Corps Development and Education Command Quantico, Virginia 22134	1

Thesis
B5422
c.1

164316

Bilodeau
Detection of signals in noise using single channel receivers.